Acta Cryst E CRYSTALLOGRAPHIC COMMUNICATIONS

ISSN 2056-9890

Crystal structure of *N*,*N*′-bis[3-(methylsulfanyl)-propyl]-1,8:4,5-naphthalenetetracarboxylic diimide

Juhyeon Park, Seung Heon Lee, Myong Yong Choi,* Cheol Joo Moon and Tae Ho Kim*

Department of Chemistry (BK21 plus) and Research Institute of Natural Sciences, Gyeongsang National University, Jinju 52828, Republic of Korea. *Correspondence e-mail: mychoi@gnu.ac.kr, thkim@gnu.ac.kr

Received 21 May 2019
Accepted 29 May 2019

Edited by J. Simpson, University of Otago, New Zealand

Keywords: crystal structure; naphthalenetetracarboxylic diimide; crystal packing; hydrogen bonding; DFT calculations; Hirshfeld surface analysis..

CCDC reference: 1919395

Supporting information: this article has supporting information at journals.iucr.org/e

The title compound, $C_{22}H_{22}N_2O_4S_2$, was synthesized by the reaction of 1,4,5,8-naphthalenetetracarboxylic dianhydride with 3-(methylsulfanyl)propylamine. The whole molecule is generated by an inversion operation of the asymmetric unit. This molecule has an *anti* form with the terminal methylthiopropyl groups above and below the aromatic diimide plane, where four intramolecular C—H···O and C—H···S hydrogen bonds are present and the O···H···S angle is 100.8°. DFT calculations revealed slight differences between the solid state and gas phase structures. In the crystal, C—H···O and C—H···S hydrogen bonds link the molecules into chains along the [2$\bar{2}$0] direction. adjacent chains are interconnected by π–π interactions, forming a two-dimensional network parallel to the (001) plane. Each two-dimensional layer is further packed in an *ABAB* sequence along the *c*-axis direction. Hirshfeld surface analysis shows that van der Waals interactions make important contributions to the intermolecular contacts. The most important contacts found in the Hirshfeld surface analysis are H···H (44.2%), H···O/O···H (18.2%), H···C/C···H (14.4%), and H···S/S···H (10.2%).

1. Chemical context

Naphthalene diimide, which has an expanded π-electron-deficient plane has attracted considerable interest as an excellent organic linker material for the production of photochromic coordination polymers as a result of their photoinduced electron transfer from neutral organic moieties to stable anionic radicals (Liu *et al.*, 2018). Aromatic imides are highly fluorescent residues that are used in the signal generation of sensors or on–off molecular switches. They have also been used in the design of receptors (Claudio-Catalán *et al.*, 2016) and sensors to recognize charged species and other guests (Landey-Álvarez *et al.*, 2016). In addition, naphthalene diimides are ideal for studying anionic···π interactions because the quadrupole moments are highly positive (Fang *et al.*, 2015). We have extended our work on naphthalene diimides to produce the title compound by the reaction of naphthalenecarboxylic dianhydride with methylthiopyrimidine and report its crystal structure here.

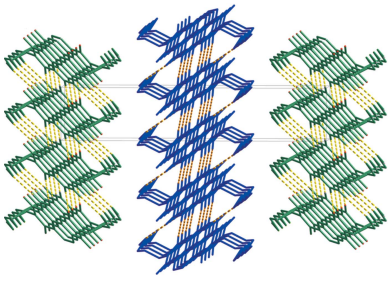

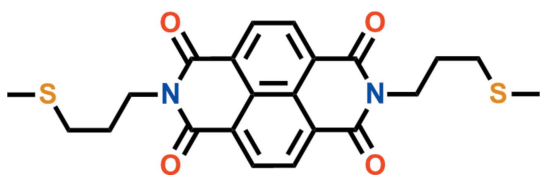

OPEN ACCESS

Table 1
Hydrogen-bond geometry (Å, °).

D—H···A	D—H	H···A	D···A	D—H···A
C4—H4A···S1	0.99	2.84	3.300 (2)	109
C4—H4A···O1	0.99	2.32	2.688 (3)	101
C10—H10···O1^{i}	0.95	2.39	3.316 (3)	164
C11—H11···S1^{ii}	0.95	2.86	3.779 (2)	162

Symmetry codes: (i) $-x+1, -y, -z$; (ii) $x+1, y+1, z$.

2. Structural commentary

The title compound comprises a central naphthalene diimide with terminal thiopropyl chains (Fig. 1). The molecule lies on a crystallographic inversion center located at the centroid of the naphthalene ring system and the asymmetric unit is composed of one half of the molecule. As expected, the naphthalene diimide plane (N1/C5/O1/C6/C10/C7/C8/C11/C9/O2) is roughly planar with an r.m.s. deviation of 0.024 Å. The total distance between the terminal carbon atoms is 18.621 Å. Furthermore, this molecule has an *anti* form as a result of the intramolecular C4—H4A···O1 and C4—H4A···S1 hydrogen bonds (Table 1). The terminal methylthiopropylamine group is fixed at an O1···H4A···S1 angle of 100.8° by the aforementioned intramolecular hydrogen bonds. The C3/C2/S1/C1 section of the methylthiopropyl substituent is almost parallel to the naphthalene diimide unit with the C3/C2/S1/C1 mean plane inclined to the naphthalene diimide plane at a dihedral angle of 13.1 (2)°.

3. Theoretical calculations

DFT calculations were performed using the *GAUSSIAN09* software package (Frisch *et al.*, 2009) and the calculated distances and angles were compared with experimental values from the X-ray diffraction studies. The overall structural calculation was performed using the B3LYP level theory with a 6–311^{++}G** basis set. The parameters optimized for bond lengths and bond angles are in close agreement with experimental crystallographic data (Table 2). The terminal methylthiopropyl group is fixed by internal hydrogen bonding in the crystal, whereas its internal hydrogen bonds are broken in the gas-phase structural calculation. This can be confirmed by the fact that the O1···H4A···S1 angle of the methylthiopropyl group has changed from 100.8 to 122.0° (Fig. 2). However, even in the gas phase the molecule has an *anti* form similar to that found in the solid state.

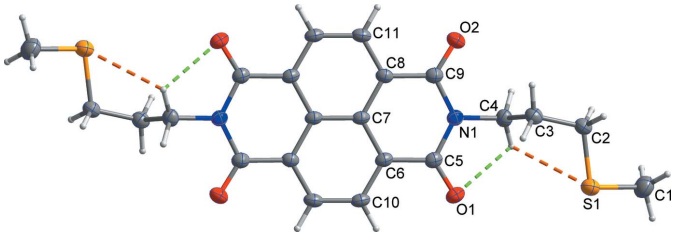

Figure 1
The asymmetric unit of the title compound, with displacement ellipsoids drawn at the 50% probability level. H atoms are shown as small spheres of arbitrary radius and yellow and green dashed lines represent intramolecular C—H···S and C—H···O hydrogen bonds, respectively. Unlabelled atoms are generated by the symmetry operation ($-x+2, -y+1, -z$).

Table 2
Experimental and calculated bond lengths (Å).

Bond	X-ray	B3LYP (6–311++G**)
O1—C5	1.210 (3)	1.2158
O2—C9	1.221 (3)	1.2173
N1—C4	1.471 (3)	1.4779
N1—C5	1.404 (3)	1.4047
N1—C9	1.394 (3)	1.4029
S1—C1	1.785 (3)	1.8244
S1—C2	1.803 (2)	1.8399
C2—C3	1.523 (3)	1.5301
C3—C4	1.521 (3)	1.5341
C5—C6	1.479 (3)	1.4880
C6—C7	1.408 (3)	1.4135
C7—C8	1.415 (3)	1.4136
C8—C9	1.478 (3)	1.4877
C6—C10	1.381 (3)	1.3835
C8—C11	1.373 (3)	1.3835

4. Supramolecular features

In the crystal, C—H···O and C—H···S hydrogen bonds (Table 1) link the molecules, forming $R_2^2(11)$ and $R_2^2(10)$ rings (Fig. 3) and resulting in chains along the [2$\bar{2}$0] direction. Adjacent chains are linked by intermolecular π–π interactions between naphthalene diimide rings [$Cg1\cdots Cg2$ = 3.5756 (12) Å; $Cg1$ and $Cg2$ are the centroids of the C6/C7/C7^{iii}/C8^{iii}/C10/C11^{iii} and C6^{iv}/C7^{iv}/C7^{v}/C8^{v}/C10^{iv}/C11^{v} rings, respectively; symmetry codes: (iii) $-x+2, -y+1, -z$; (iv) $-x+2, -y, -z$; (v) $x, y-1, z$]. These π–π interactions lead to a two-dimensional network structure parallel to the (001) plane (Fig. 4). The network structures are stacked in an alternating *ABAB* sequence along the *c*-axis direction (Fig. 5).

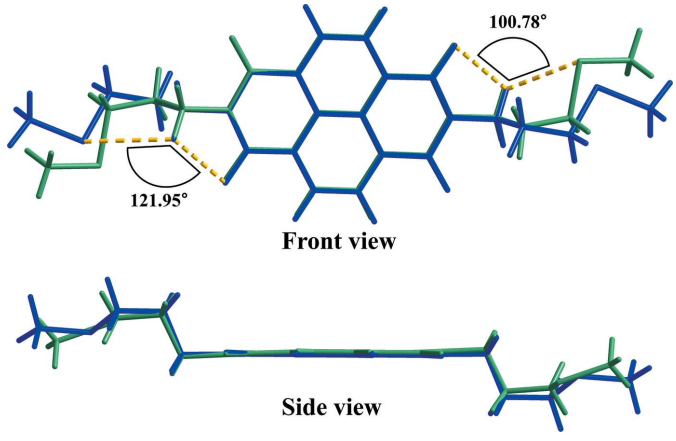

Figure 2
Atom-by-atom superimposition of the calculated structure (blue) using B3LYP/6–311^{++}G** and the X-ray structure (green) for the title compound.

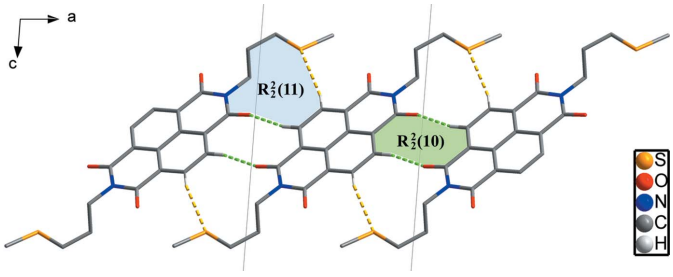

Figure 3
Intermolecular C—H···S and C—H···O hydrogen bonds (yellow and green dashed lines) forming chains along the [2$\bar{2}$0] direction with $R_2^2(11)$ and $R_2^2(10)$ motifs.

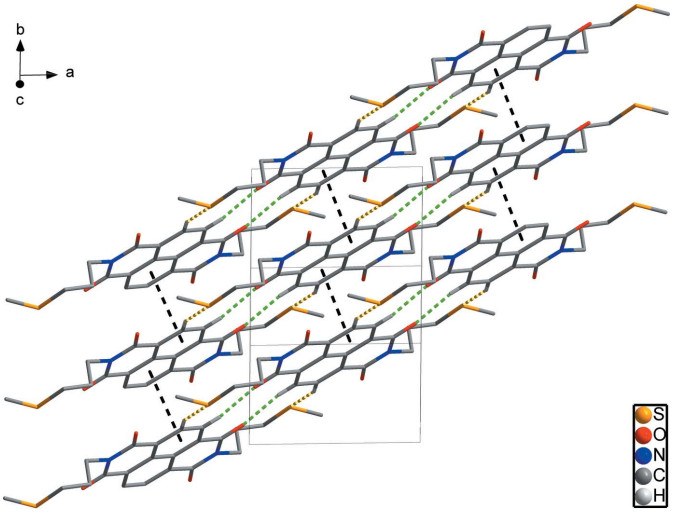

Figure 4
A packing diagram for the title compound, showing the two-dimensional network formed by C—H···S and C—H···O hydrogen bonds (yellow and green dashed lines) and π–π interactions (black dashed lines). H atoms not involved in intermolecular interactions have been omitted for clarity.

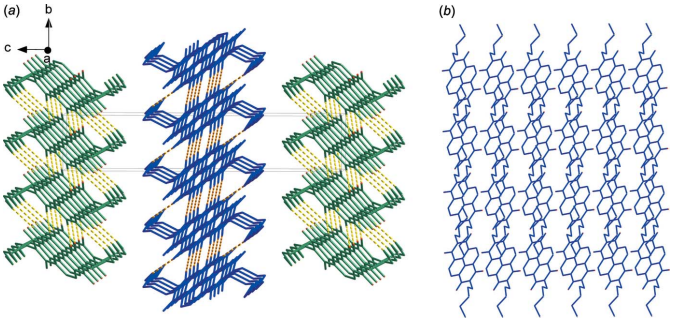

Figure 5
Packing diagrams of the title compound showing (*a*) the *ABAB* stacking pattern and (*b*) the two-dimensional structure.

5. Hirshfeld surface analysis

Hirshfeld surface analysis was performed using *CrystalExplorer* (Turner *et al.*, 2017) to quantify the various intermolecular interactions in the molecular packing of the title compound. The bright red dots in Fig. 6 showing the Hirshfeld surface mapped to the normalized contact distance (d_{norm}) indicate the $R_2^2(11)$ and $R_2^2(10)$ loops, and the contact points of the intermolecular C—H···O and C—H···S hydrogen bonds. The lighter red dot on the surface represents the π–π interaction with adjacent molecules. The white and blue colours that make up the majority of the surface indicate contact distances that are equal to or greater than the van der Waals radii.

Table 3
Percentage contributions of interatomic contacts to the Hirshfeld surface of the title compound..

Contact	Percentage contribution
H···H	44.2
H···O/O···H	18.3
H···C/C···H	14.4
H···S/S···H	10.2
C···O/O···C	5.6
C···C	4.5
H···N/N···H	1.4
O···O	0.5
N···O/O···N	0.4
C···S/S···C	0.4

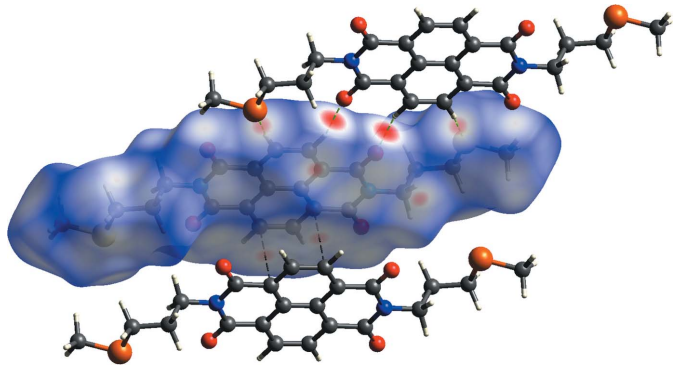

Figure 6
A view of the Hirshfeld surface of the title compound mapped over d_{norm}, showing the H···S and H···O contacts of the intermolecular interactions using a fixed colour scale of −0.2580 (red) to 1.0789 (blue) a.u.

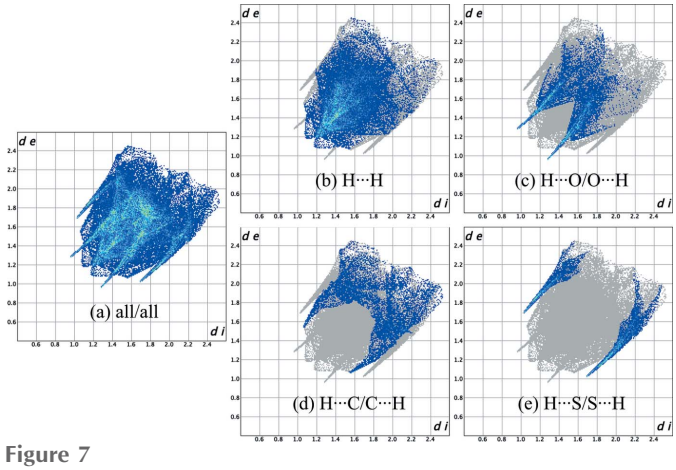

Figure 7
(*a*) The full two-dimensional fingerprint plot for the title compound and those delineated into (*b*) H···H, (*c*) H···O/O···H, (*d*) H···C/C···H and (*e*) H···S/S···H contacts. The d_i and d_e values are the closest internal and external distances (in Å) from given points on the Hirshfeld surface contacts.

The C—H···O and C—H···S hydrogen bonds and π–π stacking interactions are identified in the two-dimensional fingerprint plots (Fig. 7*a*–*e*), which show the H···H, H···C/C···H, H···O/O···H, H···N/N···H, and H···S/S···H contacts. The relative contributions of the atomic contacts to the Hirshfeld surface are summarized in Table 3. These show that the dominant interaction, accounting for 44.2% of the surface, is the H···H van der Waals interaction. Substantial contributions are also made by H···O/O···H (18.3%), H···C/C···H (14.4%), and H···S/S···H (10.2%) contacts, which are indicated by two sharp peaks in each fingerprint plot. Lesser contributions from C···O/O···C, C···C, H···N/N···H, O···O, N···O/O···N, and C···S/S···C contacts are included in Table 3 for completeness.

6. Synthesis and crystallization

A mixture of 1,4,5,8-naphthalenetetracarboxylic dianhydride (6.70 g, 25.0 mmol) and 3-(methylsulfanyl)propylamine (5.6 mL, 50.0 mmol) in toluene (5 mL) and quinoline (15 mL) was heated at 453 K with stirring for 1h. Upon cooling to room temperature, a golden yellow crude solid was filtered off and washed with diethyl ether. A golden yellow powder was obtained. Crystals suitable for X-ray diffraction analysis were obtained by slow evaporation of a dichloromethane solution of the title compound.

^{1}H NMR (300 MHz, $CDCl_3$): δ 8.77 (*s*, 2H, Ar), 4.33 (*t*, 2H, CH_2N), 2.64 (*t*, 2H, CH_2), 2.14 (*s*, 3H, CH_3), 2.07 (*t*, 2H, CH_2S). ^{13}C NMR (75.4 MHz, $CDCl_3$): δ 162.81, 130.99, 126.69, 126.57, 40.01, 31.61, 27.16 and 15.31. IR (ν, cm^{-1}): 3344 (*m*); 3071 (*m*); 2916 (*s*); 2848 (*s*); 1999 (*s*); 1693 (*s*).

7. Database survey

A search of the Cambridge Structural Database (CSD, Version 5.40, updated February 2019; Groom *et al.*, 2016) for naphthalene diimide derivatives gave 31 hits for structures that include a terminal propyl group. The title compound was not found. Related compounds include a series of cycloalkyl-substituted naphthalene tetracarboxylic diimides (Kakinuma *et al.*, 2013). Other terminal *n*-alkyl groups are known with 2,7-dibutylbenzo[*lmn*][3,8]phenanthroline-1,3,6,8-tetraone (Alvey *et al.*, 2010), bis-*N*,*N*′-dipentylnaphthalene-1,4,5,8-tetracarboxylic diimide (Andric *et al.*, 2004), *N*,*N*′-di-*n*-hexyl-1,4;5,8-naphthalenetetracarboxylic diimide (Ofir *et al.*, 2006), and *N*,*N*′-di(*n*-dodecyl)naphthalene-4,5,8,9-tetracarboxylic acid diimide (Kozycz *et al.*, 2015).

8. Refinement

Crystal data, data collection and structure refinement details are summarized in Table 4. All H atoms were positioned geometrically and refined using a riding model with d(C—H) = 0.95 Å, U_{iso} = 1.2U_{eq}(C) for aromatic, d(C—H) = 0.99 Å, U_{iso} = 1.2U_{eq}(C) for methylene, and d(C—H) = 0.98 Å, U_{iso} = 1.5U_{eq}(C) for the methyl H atoms.

Table 4
Experimental details.

Crystal data	
Chemical formula	$C_{22}H_{22}N_2O_4S_2$
M_r	442.53
Crystal system, space group	Monoclinic, $P2_1/c$
Temperature (K)	173
a, b, c (Å)	8.0500 (2), 4.9407 (1), 24.9626 (7)
β (°)	94.333 (2)
V (Å^3)	989.99 (4)
Z	2
Radiation type	Mo $K\alpha$
μ (mm^{-1})	0.30
Crystal size (mm)	0.23 × 0.05 × 0.04
Data collection	
Diffractometer	Bruker APEXII CCD
Absorption correction	Multi-scan (*SADABS*; Bruker, 2014)
T_{min}, T_{max}	0.676, 0.746
No. of measured, independent and observed [$I > 2\sigma(I)$] reflections	5641, 1732, 1360
R_{int}	0.046
(sin $\theta/\lambda)_{max}$ (Å^{-1})	0.595
Refinement	
$R[F^2 > 2\sigma(F^2)]$, $wR(F^2)$, S	0.042, 0.101, 1.05
No. of reflections	1732
No. of parameters	137
H-atom treatment	H-atom parameters constrained
$\Delta\rho_{max}$, $\Delta\rho_{min}$ (e Å^{-3})	0.25, −0.26

Computer programs: *APEX2* and *SAINT* (Bruker, 2014), *SHELXS97* and *SHELXTL* (Sheldrick, 2008), *SHELXL2014* (Sheldrick, 2015), *DIAMOND* (Brandenburg, 2010) and *publCIF* (Westrip, 2010).

Acknowledgements

The authors thank Dr J.-E. Lee of the Central Research Facilities for her assistance with the NMR and XRD experiments.

Funding information

This research was supported by the Basic Science Research Program through the National Research Foundation of Korea (NRF) funded by the Ministry of Education, Science and Technology (grant Nos. 2017M2B2A9A020049940 and 2018R1D1A3B07042615).

References

Alvey, P. M., Reczek, J. J., Lynch, V. & Iverson, B. L. (2010). *J. Org. Chem.* **75**, 7682–7690.
Andric, G., Boas, J. F., Bond, A. M., Fallon, G. D., Ghiggino, K. P., Hogan, C. F., Hutchison, J. A., Lee, M. A.-P., Langford, S. J., Pilbrow, J. R., Troup, G. J. & Woodward, C. P. (2004). *Aust. J. Chem.* **57**, 1011–1019.
Brandenburg, K. (2010). *DIAMOND*. Crystal Impact GbR, Bonn, Germany.
Bruker (2014). *APEX2*, *SAINT* and *SADABS*. Bruker AXS Inc., Madison, Wisconsin, USA.
Claudio-Catalán, M. Á., Medrano, F., Tlahuext, H. & Godoy-Alcántar, C. (2016). *Acta Cryst.* E**72**, 1503–1508.
Fang, X., Guo, M.-D., Weng, L.-J., Chen, Y. & Lin, M.-J. (2015). *Dyes & Pigments*, **113**, 251–256.
Frisch, M. J., Trucks, G. W., Schlegel, H. B., Scuseria, G. E., Robb, M. A., Cheeseman, J. R., Scalmani, G., Barone, V., Mennucci, B., Petersson, G. A., Nakatsuji, H., Caricato, M., Li, X., Hratchian,

H. P., Izmaylov, A. F., Bloino, J., Zheng, G., Sonnenberg, J. L., Hada, M., Ehara, M., Toyota, K., Fukuda, R., Hasegawa, J., Ishida, M., Nakajima, T., Honda, Y., Kitao, O., Nakai, H., Vreven, T., Montgomery, J. J. A., Peralta, J. E., Ogliaro, F., Bearpark, M., Heyd, J. J., Brothers, E., Kudin, K. N., Staroverov, V. N., Kobayashi, R., Normand, J., Raghavachari, K., Rendell, A., Burant, J. C., Iyengar, S. S., Tomasi, J., Cossi, M., Rega, N., Millam, J. M., Klene, M., Knox, J. E., Cross, J. B., Bakken, V., Adamo, C., Jaramillo, J., Gomperts, R., Stratmann, R. E., Yazyev, O., Austin, A. J., Cammi, R., Pomelli, C., Ochterski, J. W., Martin, R. L., Morokuma, K., Zakrzewski, V. G., Voth, G. A., Salvador, P., Dannenberg, J. J., Dapprich, S., Daniels, A. D., Farkas, O., Foresman, J. B., Ortiz, J. V., Cioslowski, J. & Fox, D. J. (2009). *Gaussian09*. Gaussian Inc, Wallingford, Connecticut, USA.

Groom, C. R., Bruno, I. J., Lightfoot, M. P. & Ward, S. C. (2016). *Acta Cryst.* B**72**, 171–179.

Kakinuma, T., Kojima, H., Ashizawa, M., Matsumoto, H. & Mori, T. (2013). *J. Mater. Chem. C.* **1**, 5395–5401.

Kozycz, L. M., Guo, C., Manion, J. G., Tilley, A. J., Lough, A. J., Li, Y. & Seferos, D. S. (2015). *J. Mater. Chem. C.* **3**, 11505–11515.

Landey-Álvarez, M. A., Ochoa-Terán, A., Pina-Luis, G., Martínez-Quiroz, M., Aguilar-Martínez, M., Elías-García, J., Miranda-Soto, V., Ramírez, J.-Z., Machi-Lara, L., Labastida-Galván, V. & Ordoñez, M. (2016). *Supramol. Chem.* **28**, 892–906.

Liu, J.-J., Dong, Y., Chen, L.-Z., Wang, L., Xia, S.-B. & Huang, C.-C. (2018). *Acta Cryst.* C**74**, 94–99.

Ofir, Y., Zelichenok, A. & Yitzchaik, S. (2006). *J. Mater. Chem.* **16**, 2142–2149.

Sheldrick, G. M. (2008). *Acta Cryst.* A**64**, 112–122.

Sheldrick, G. M. (2015). *Acta Cryst.* C**71**, 3–8.

Turner, M. J., MacKinnon, J. J., Wolff, S. K., Grimwood, D. J., Spackman, P. R., Jayatilaka, D. & Spackman, M. A. (2017). *Crystal Explorer17.5*. University of Western Australia, Perth.

Westrip, S. P. (2010). *J. Appl. Cryst.* **43**, 920–925.

supporting information

Acta Cryst. (2019). E**75**, 934-938 [https://doi.org/10.1107/S2056989019007771]

Crystal structure of *N*,*N*′-bis[3-(methylsulfanyl)propyl]-1,8:4,5-naphthalenetetracarboxylic diimide

Juhyeon Park, Seung Heon Lee, Myong Yong Choi, Cheol Joo Moon and Tae Ho Kim

Computing details

Data collection: *APEX2* (Bruker, 2014); cell refinement: *SAINT* (Bruker, 2014); data reduction: *SAINT* (Bruker, 2014); program(s) used to solve structure: *SHELXS97* (Sheldrick, 2008); program(s) used to refine structure: *SHELXL2014* (Sheldrick, 2015); molecular graphics: *DIAMOND* (Brandenburg, 2010); software used to prepare material for publication: *SHELXTL* (Sheldrick, 2008) and *publCIF* (Westrip, 2010).

N,*N*′-Bis[3-(methylsulfanyl)propyl]-1,8:4,5-naphthalenetetracarboxylic diimide

Crystal data

$C_{22}H_{22}N_2O_4S_2$
M_r = 442.53
Monoclinic, $P2_1/c$
a = 8.0500 (2) Å
b = 4.9407 (1) Å
c = 24.9626 (7) Å
β = 94.333 (2)°
V = 989.99 (4) Å^3
Z = 2
$F(000)$ = 464
D_x = 1.485 Mg m^{-3}
Mo $K\alpha$ radiation, λ = 0.71073 Å
Cell parameters from 1676 reflections
θ = 3.1–26.1°
μ = 0.30 mm^{-1}
T = 173 K
Rod, yellow
0.23 × 0.05 × 0.04 mm

Data collection

Bruker APEXII CCD diffractometer
φ and ω scans
Absorption correction: multi-scan (SADABS; Bruker, 2014)
T_{min} = 0.676, T_{max} = 0.746
5641 measured reflections
1732 independent reflections
1360 reflections with $I > 2\sigma(I)$
R_{int} = 0.046
θ_{max} = 25.0°, θ_{min} = 1.6°
h = −9→9
k = −5→5
l = −29→25

Refinement

Refinement on F^2
Least-squares matrix: full
$R[F^2 > 2\sigma(F^2)]$ = 0.042
$wR(F^2)$ = 0.101
S = 1.05
1732 reflections
137 parameters
0 restraints
Hydrogen site location: inferred from neighbouring sites
H-atom parameters constrained
$w = 1/[\sigma^2(F_o^2) + (0.0403P)^2 + 0.3426P]$ where $P = (F_o^2 + 2F_c^2)/3$
$(\Delta/\sigma)_{max} < 0.001$
$\Delta\rho_{max}$ = 0.25 e Å^{-3}
$\Delta\rho_{min}$ = −0.26 e Å^{-3}

Special details

Geometry. All esds (except the esd in the dihedral angle between two l.s. planes) are estimated using the full covariance matrix. The cell esds are taken into account individually in the estimation of esds in distances, angles and torsion angles; correlations between esds in cell parameters are only used when they are defined by crystal symmetry. An approximate (isotropic) treatment of cell esds is used for estimating esds involving l.s. planes.

Fractional atomic coordinates and isotropic or equivalent isotropic displacement parameters (Å²)

	x	*y*	*z*	U_{iso}*/U_{eq}
S1	0.25895 (9)	0.32924 (13)	0.17605 (3)	0.0356 (2)
O1	0.5336 (2)	0.2804 (3)	0.04996 (7)	0.0310 (4)
O2	0.8407 (2)	0.9669 (3)	0.12693 (6)	0.0326 (5)
N1	0.6852 (2)	0.6297 (4)	0.08708 (8)	0.0243 (5)
C1	0.0764 (4)	0.4611 (6)	0.20299 (12)	0.0458 (8)
H1A	0.0888	0.4506	0.2423	0.069*
H1B	−0.0207	0.3548	0.1895	0.069*
H1C	0.0609	0.6503	0.1919	0.069*
C2	0.4130 (3)	0.5621 (5)	0.20506 (10)	0.0273 (6)
H2A	0.3685	0.7488	0.2024	0.033*
H2B	0.4374	0.5191	0.2436	0.033*
C3	0.5728 (3)	0.5448 (5)	0.17623 (9)	0.0276 (6)
H3A	0.6650	0.6315	0.1985	0.033*
H3B	0.6023	0.3526	0.1710	0.033*
C4	0.5500 (3)	0.6857 (5)	0.12200 (10)	0.0274 (6)
H4A	0.4431	0.6269	0.1035	0.033*
H4B	0.5434	0.8834	0.1279	0.033*
C5	0.6592 (3)	0.4151 (4)	0.05056 (9)	0.0243 (6)
C6	0.7912 (3)	0.3668 (4)	0.01356 (9)	0.0214 (5)
C7	0.9374 (3)	0.5241 (4)	0.01778 (8)	0.0200 (5)
C8	0.9613 (3)	0.7304 (4)	0.05690 (9)	0.0228 (5)
C9	0.8287 (3)	0.7878 (4)	0.09317 (9)	0.0249 (6)
C10	0.7698 (3)	0.1661 (4)	−0.02484 (9)	0.0234 (5)
H10	0.6712	0.0598	−0.0273	0.028*
C11	1.1054 (3)	0.8802 (4)	0.06017 (9)	0.0242 (6)
H11	1.1210	1.0173	0.0868	0.029*

Atomic displacement parameters (Å²)

	U^{11}	U^{22}	U^{33}	U^{12}	U^{13}	U^{23}
S1	0.0366 (5)	0.0304 (4)	0.0400 (4)	−0.0049 (3)	0.0038 (3)	−0.0064 (3)
O1	0.0268 (11)	0.0293 (9)	0.0371 (10)	−0.0088 (8)	0.0036 (8)	−0.0010 (8)
O2	0.0372 (11)	0.0284 (9)	0.0322 (10)	−0.0041 (8)	0.0025 (8)	−0.0113 (8)
N1	0.0252 (12)	0.0200 (10)	0.0273 (11)	−0.0021 (9)	0.0009 (9)	−0.0004 (8)
C1	0.0360 (19)	0.0483 (17)	0.0541 (19)	−0.0024 (14)	0.0104 (14)	0.0018 (15)
C2	0.0320 (16)	0.0220 (12)	0.0276 (13)	−0.0002 (11)	−0.0003 (11)	−0.0003 (10)
C3	0.0292 (15)	0.0272 (13)	0.0260 (13)	0.0017 (11)	−0.0011 (11)	−0.0019 (10)
C4	0.0254 (15)	0.0255 (13)	0.0314 (14)	0.0034 (11)	0.0038 (11)	0.0005 (11)
C5	0.0275 (15)	0.0199 (12)	0.0247 (13)	−0.0006 (11)	−0.0034 (10)	0.0039 (10)

C6	0.0237 (14)	0.0150 (11)	0.0248 (13)	0.0001 (10)	−0.0031 (10)	0.0028 (9)
C7	0.0226 (14)	0.0152 (11)	0.0214 (12)	−0.0006 (10)	−0.0037 (9)	0.0028 (9)
C8	0.0253 (14)	0.0178 (11)	0.0246 (13)	−0.0015 (10)	−0.0026 (10)	0.0028 (9)
C9	0.0284 (15)	0.0211 (12)	0.0246 (13)	0.0008 (10)	−0.0021 (10)	0.0034 (10)
C10	0.0220 (14)	0.0198 (12)	0.0273 (13)	−0.0028 (10)	−0.0065 (10)	0.0044 (10)
C11	0.0302 (15)	0.0177 (11)	0.0236 (13)	−0.0019 (10)	−0.0045 (10)	−0.0018 (9)

Geometric parameters (Å, º)

S1—C1	1.785 (3)	C3—H3B	0.9900
S1—C2	1.803 (2)	C4—H4A	0.9900
O1—C5	1.210 (3)	C4—H4B	0.9900
O2—C9	1.221 (3)	C5—C6	1.479 (3)
N1—C9	1.394 (3)	C6—C10	1.381 (3)
N1—C5	1.404 (3)	C6—C7	1.408 (3)
N1—C4	1.471 (3)	C7—C7^{i}	1.413 (4)
C1—H1A	0.9800	C7—C8	1.415 (3)
C1—H1B	0.9800	C8—C11	1.373 (3)
C1—H1C	0.9800	C8—C9	1.478 (3)
C2—C3	1.523 (3)	C10—C11^{i}	1.404 (3)
C2—H2A	0.9900	C10—H10	0.9500
C2—H2B	0.9900	C11—C10^{i}	1.404 (3)
C3—C4	1.521 (3)	C11—H11	0.9500
C3—H3A	0.9900		
C1—S1—C2	100.17 (12)	N1—C4—H4B	108.9
C9—N1—C5	125.2 (2)	C3—C4—H4B	108.9
C9—N1—C4	118.31 (19)	H4A—C4—H4B	107.7
C5—N1—C4	116.52 (19)	O1—C5—N1	120.4 (2)
S1—C1—H1A	109.5	O1—C5—C6	122.9 (2)
S1—C1—H1B	109.5	N1—C5—C6	116.7 (2)
H1A—C1—H1B	109.5	C10—C6—C7	120.5 (2)
S1—C1—H1C	109.5	C10—C6—C5	119.5 (2)
H1A—C1—H1C	109.5	C7—C6—C5	120.0 (2)
H1B—C1—H1C	109.5	C6—C7—C7^{i}	119.5 (2)
C3—C2—S1	110.75 (16)	C6—C7—C8	121.3 (2)
C3—C2—H2A	109.5	C7^{i}—C7—C8	119.3 (3)
S1—C2—H2A	109.5	C11—C8—C7	120.0 (2)
C3—C2—H2B	109.5	C11—C8—C9	120.4 (2)
S1—C2—H2B	109.5	C7—C8—C9	119.6 (2)
H2A—C2—H2B	108.1	O2—C9—N1	120.2 (2)
C4—C3—C2	110.2 (2)	O2—C9—C8	122.6 (2)
C4—C3—H3A	109.6	N1—C9—C8	117.2 (2)
C2—C3—H3A	109.6	C6—C10—C11^{i}	119.7 (2)
C4—C3—H3B	109.6	C6—C10—H10	120.1
C2—C3—H3B	109.6	C11^{i}—C10—H10	120.1
H3A—C3—H3B	108.1	C8—C11—C10^{i}	121.1 (2)
N1—C4—C3	113.37 (19)	C8—C11—H11	119.5

N1—C4—H4A	108.9	C10^{i}—C11—H11	119.5
C3—C4—H4A	108.9		
C1—S1—C2—C3	−163.99 (17)	C6—C7—C8—C11	179.8 (2)
S1—C2—C3—C4	75.4 (2)	C7^{i}—C7—C8—C11	−0.3 (4)
C9—N1—C4—C3	−84.9 (2)	C6—C7—C8—C9	−1.7 (3)
C5—N1—C4—C3	94.0 (2)	C7^{i}—C7—C8—C9	178.1 (2)
C2—C3—C4—N1	−167.95 (19)	C5—N1—C9—O2	−178.5 (2)
C9—N1—C5—O1	176.4 (2)	C4—N1—C9—O2	0.3 (3)
C4—N1—C5—O1	−2.5 (3)	C5—N1—C9—C8	2.2 (3)
C9—N1—C5—C6	−4.1 (3)	C4—N1—C9—C8	−178.94 (19)
C4—N1—C5—C6	177.07 (18)	C11—C8—C9—O2	0.0 (3)
O1—C5—C6—C10	2.3 (3)	C7—C8—C9—O2	−178.4 (2)
N1—C5—C6—C10	−177.28 (19)	C11—C8—C9—N1	179.24 (19)
O1—C5—C6—C7	−177.5 (2)	C7—C8—C9—N1	0.8 (3)
N1—C5—C6—C7	3.0 (3)	C7—C6—C10—C11^{i}	−0.4 (3)
C10—C6—C7—C7^{i}	0.2 (4)	C5—C6—C10—C11^{i}	179.8 (2)
C5—C6—C7—C7^{i}	179.9 (2)	C7—C8—C11—C10^{i}	0.5 (3)
C10—C6—C7—C8	−179.9 (2)	C9—C8—C11—C10^{i}	−177.9 (2)
C5—C6—C7—C8	−0.2 (3)		

Symmetry code: (i) −*x*+2, −*y*+1, −*z*.

Hydrogen-bond geometry (Å, º)

D—H···*A*	*D*—H	H···*A*	*D*···*A*	*D*—H···*A*
C4—H4*A*···S1	0.99	2.84	3.300 (2)	109
C4—H4*A*···O1	0.99	2.32	2.688 (3)	101
C10—H10···O1^{ii}	0.95	2.39	3.316 (3)	164
C11—H11···S1^{iii}	0.95	2.86	3.779 (2)	162

Symmetry codes: (ii) −*x*+1, −*y*, −*z*; (iii) *x*+1, *y*+1, *z*.